Supplementary material

Point Set Self-Embedding

IEEE Transactions on Visualization and Computer Graphics

OVERVIEW

This supplemental material consists of the following sections:

- In Section A, we provide more visual restoration results on point sets of various structures.
- In Section B, we provide one more visual example to demonstrate the importance of the self-embedded information.
- In Section C, we provide more visual comparison results with different downsampling methods.
- In Section D, we provide more visual comparison results on inputs of varying sizes.
- In Section E, we provide more visual comparison results on large-scale real-scanned inputs.
- In Section F, we provide a visual comparison with PointLIE [1].

APPENDIX A
MORE RESTORATION VISUALIZATION RESULTS

Figures 1-3 demonstrate the restoration ability of our framework on point clouds of various geometric structures and point distributions from the uniform, random, and partial test sets, respectively. Benefited by the self-embedded information in (b), our framework restores high-quality dense point sets (c) that are very similar to the originals, regardless of the point distribution of the inputs (a).

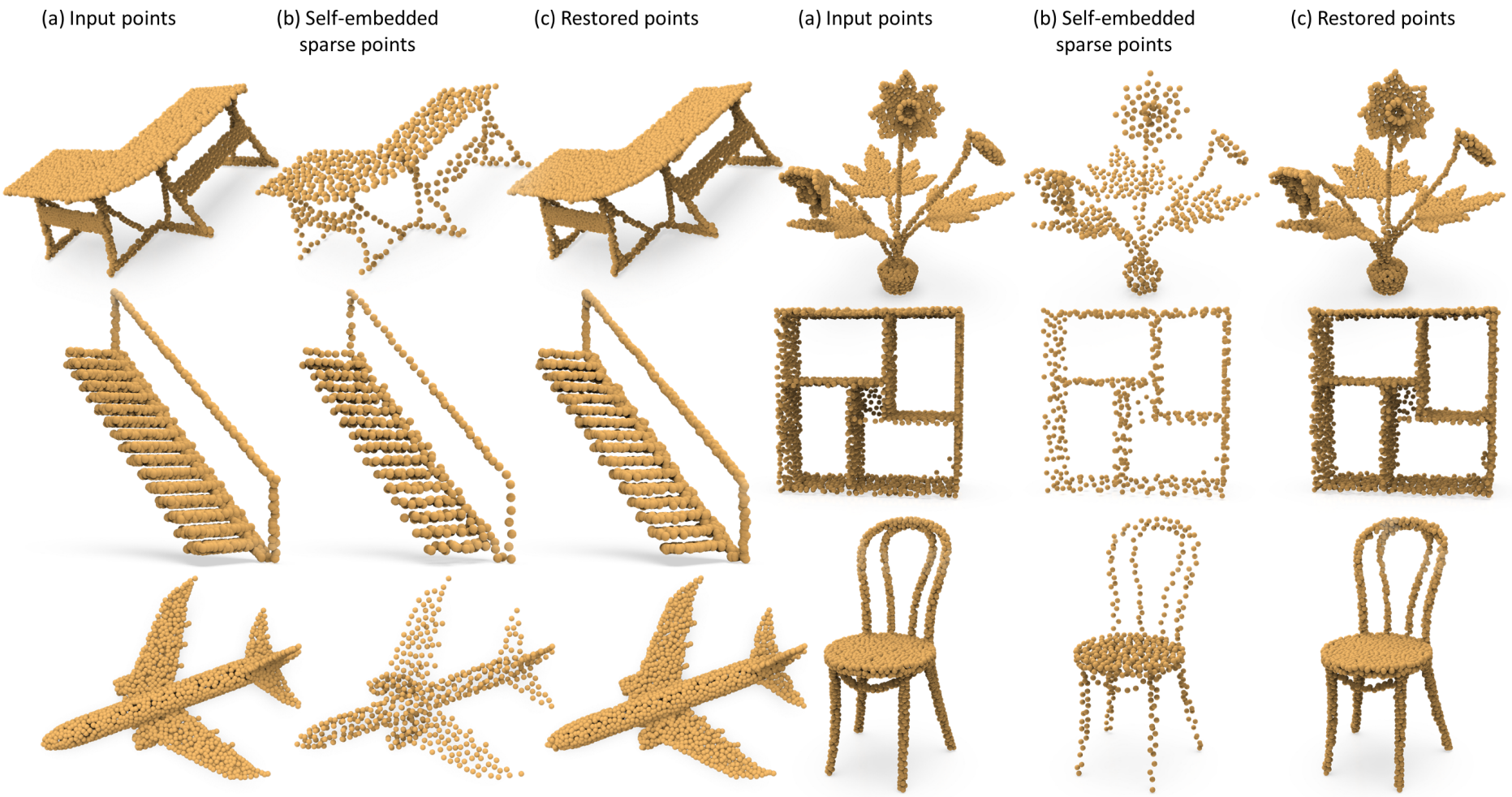


Fig. 1. Gallery of our restoration results on the *uniform set*. Given the original inputs (a), our method produces the self-embedded sparse points (b) and leverages the embedded information to achieve high-quality restorations (c).

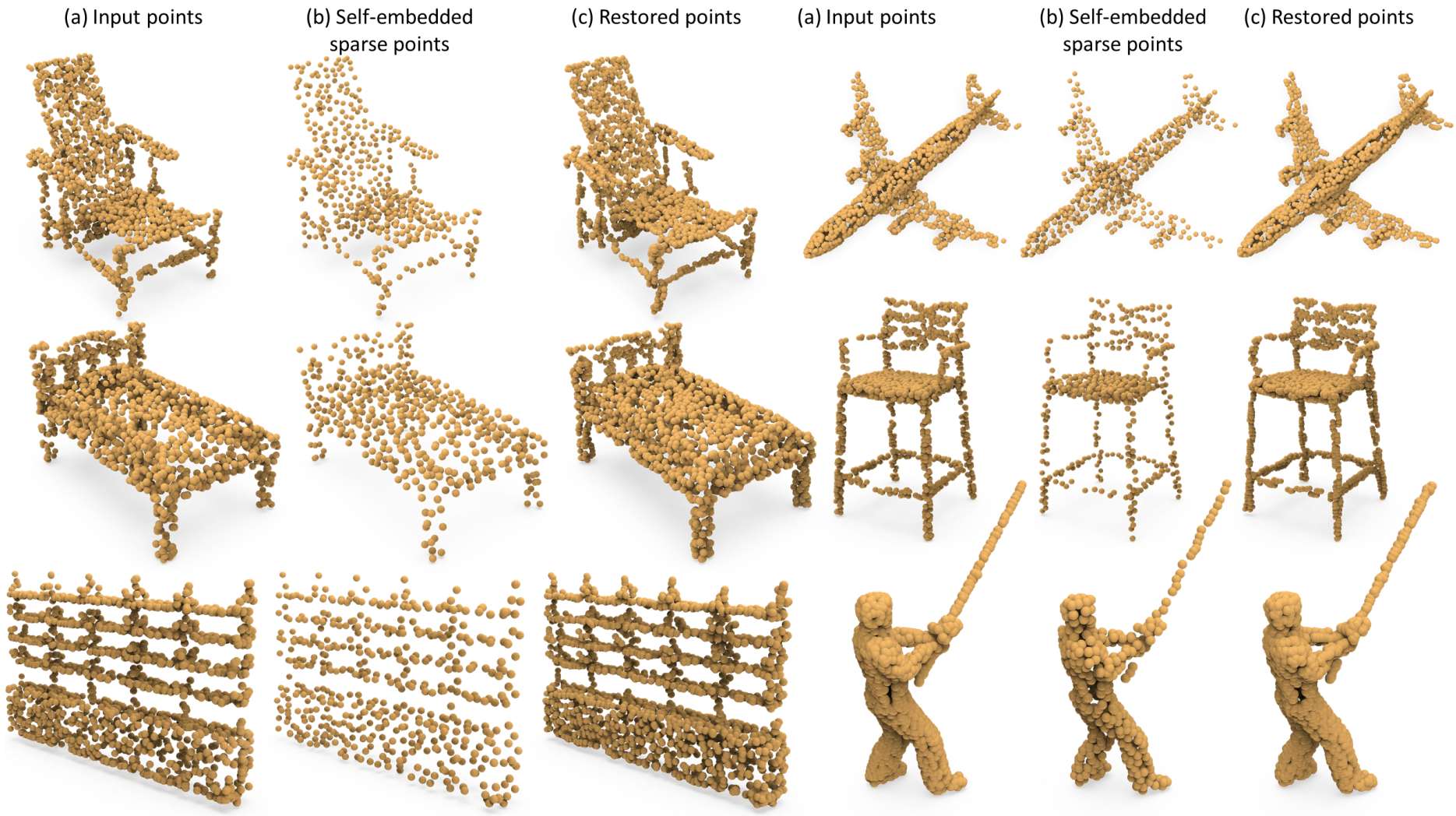


Fig. 2. Gallery of our restoration results on the *random set*. Given the original inputs (a), our method produces the self-embedded sparse points (b) and leverages the embedded information to achieve high-quality restorations (c).

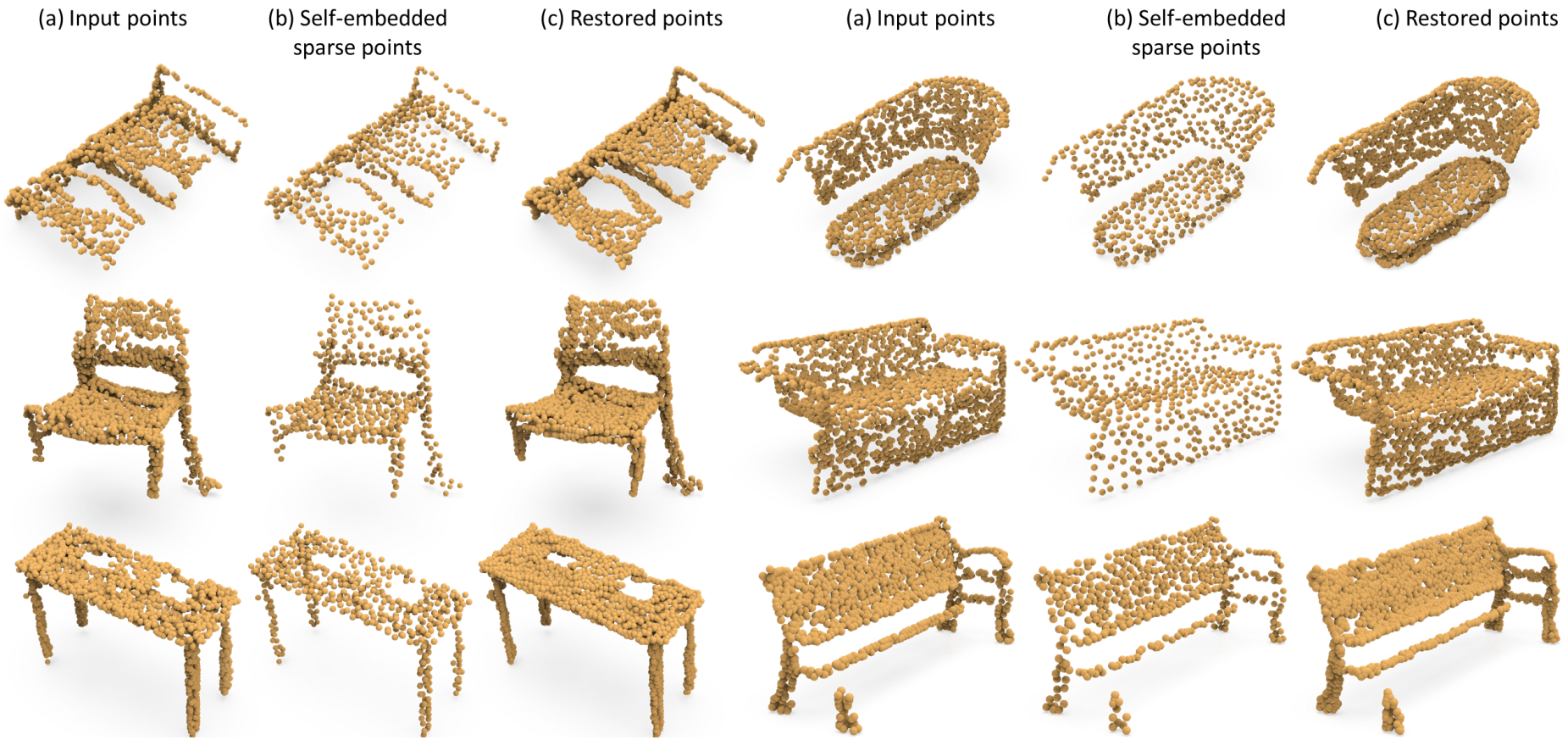


Fig. 3. Gallery of our restoration results on the *partial set*. Given the original inputs (a), our method produces the self-embedded sparse points (b) and leverages the embedded information to achieve a high-quality restoration (c).

APPENDIX B
MORE VISUAL ANALYSIS ON SELF-EMBEDDED INFORMATION

Figure 4 shows one more visual result to demonstrate the importance of the self-embedded information in the restoration. Please refer to Section 4.6 in the main paper for a detailed description.

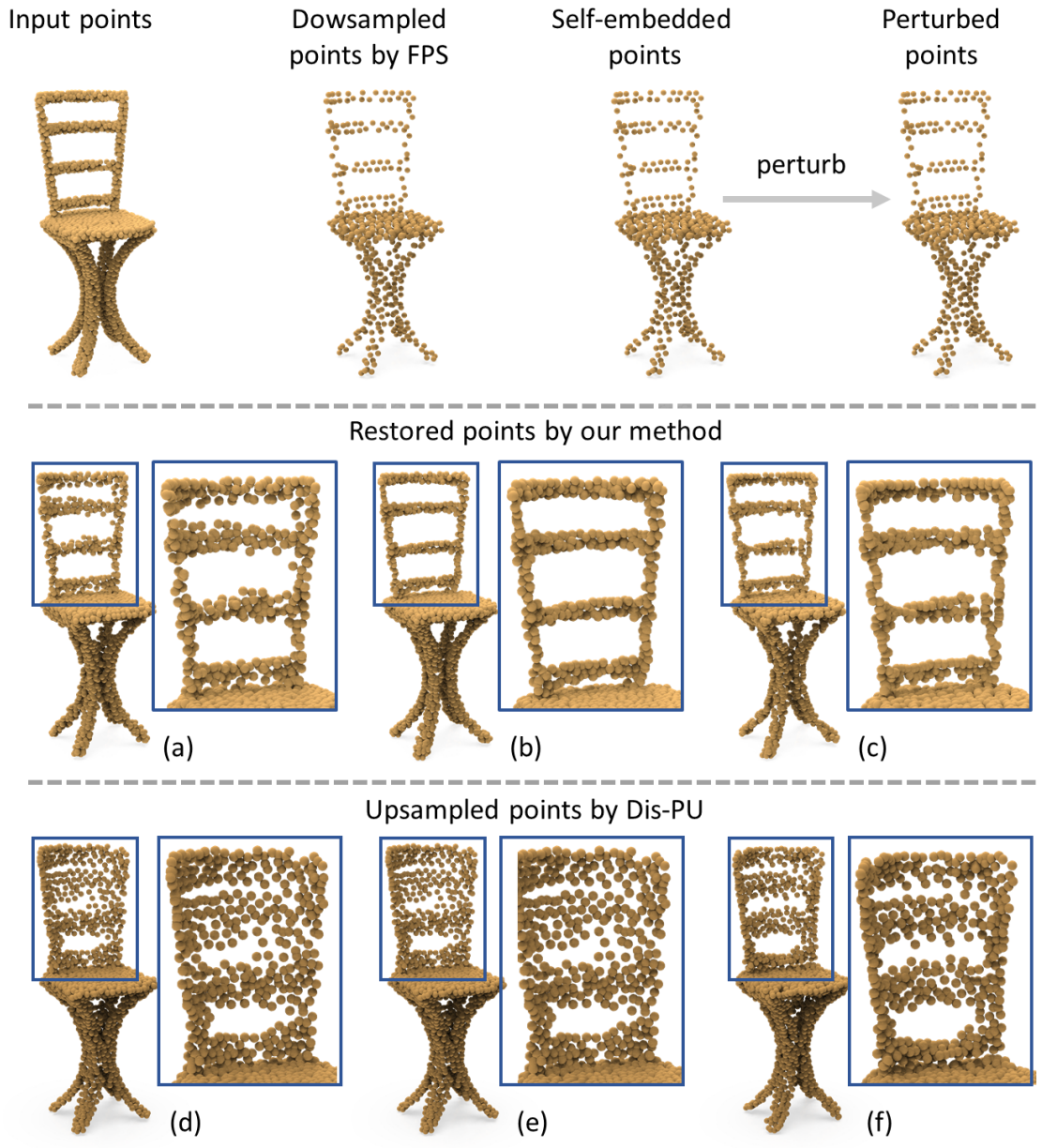


Fig. 4. Top row, from left to right: input points, downsampled points via FPS, our self-embedded points, and perturbed self-embedded points, (a)-(c) show restoration results produced by our methods, correspondingly from the three sparse inputs on the top row, whereas (d)-(f) show the corresponding upsampled points by Dis-PU [2]. We can see that the point set restored from our self-embedded points (b) achieve the best restoration vs. other results, showing the importance of the self-embedded information and that our method is able to consume the self-embedded information to produce the high-quality restoration.

APPENDIX C
COMPARISON RESULTS WITH DOWNSAMPLING METHODS

Figure 5 shows one more comparison result with FPS and SampleNet [3] (corresponding also to Figure 7 in the main paper).

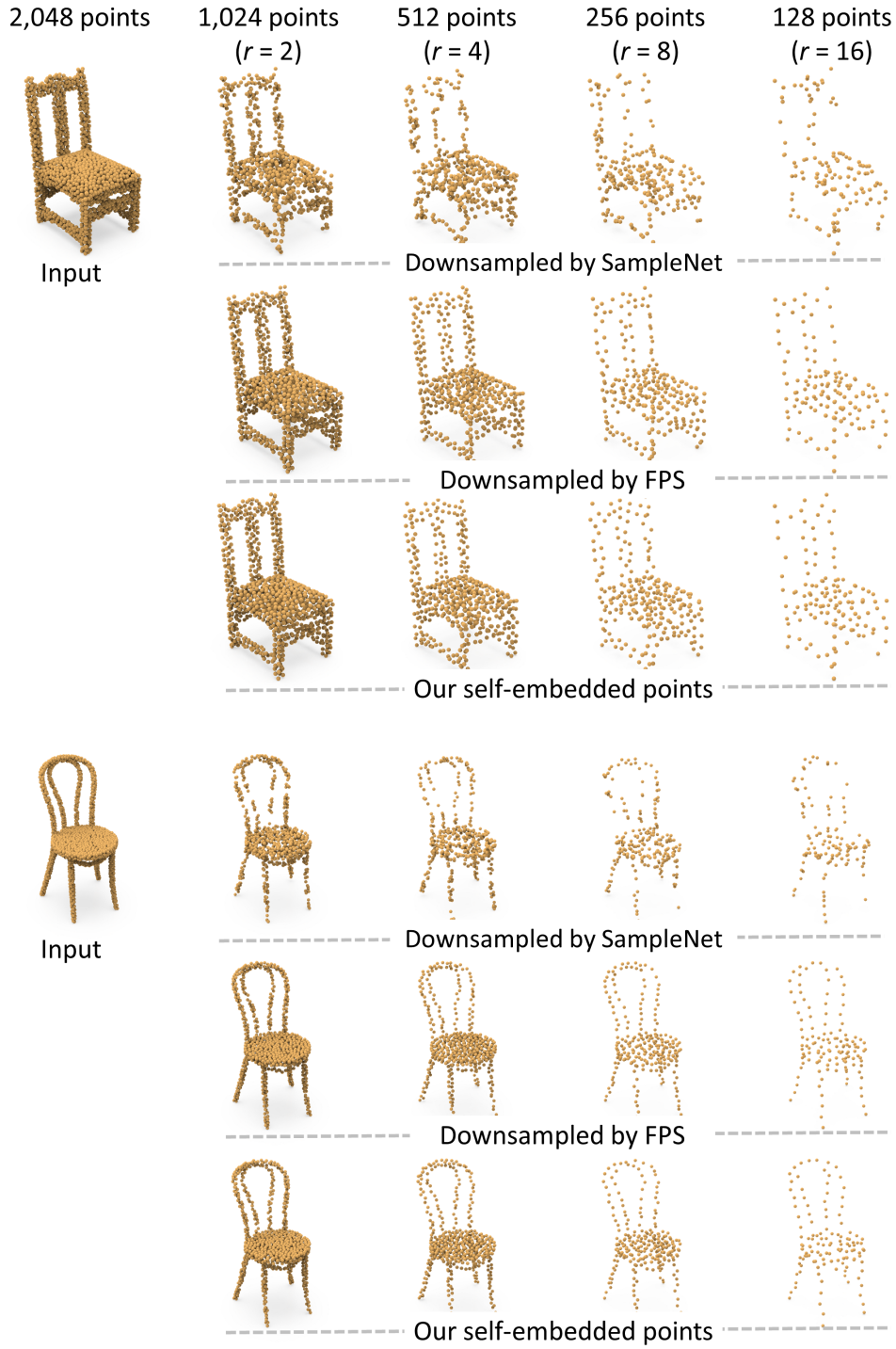


Fig. 5. Comparing the downsampling results produced by SampleNet [3] (top), FPS (middle), and our method (bottom) for decreasing sampling rates. Our self-embedded point sets are more similar to those produced by the ordinary FPS, presenting visually-recognizable shapes as the originals. In contrast, it is harder to recognize the results of SampleNet, particularly for large downsampling rates.

APPENDIX D
MORE COMPARISON RESULTS IN INPUTS OF VARYING SIZES

Figure 6 shows two more restoration results on restoring point sets of varying sizes (additional to Figure 11 in main paper). The results show that our method performs stably for varying input sizes.

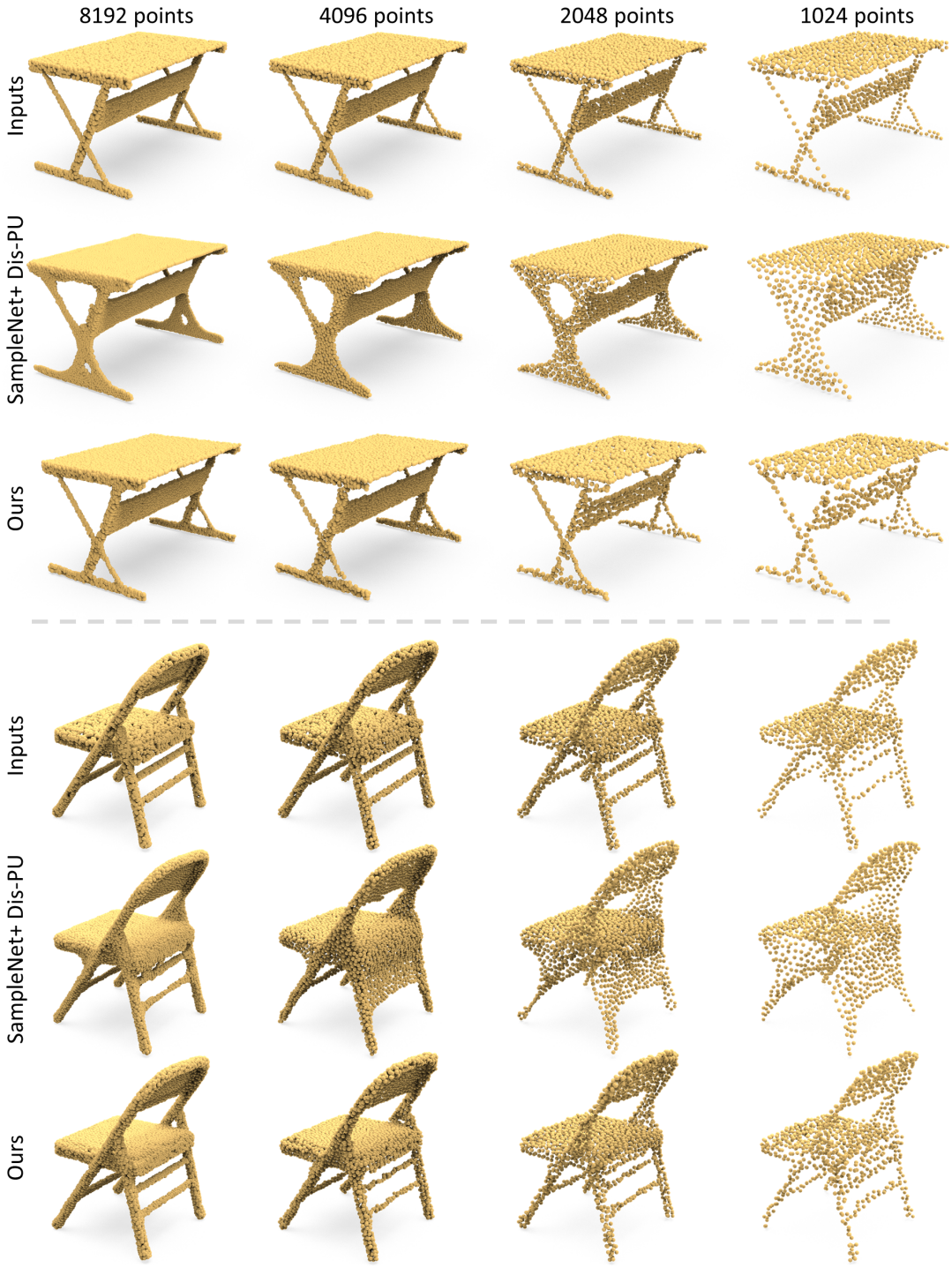


Fig. 6. Restoration results on input point sets of varying sizes (left to right).

APPENDIX E
MORE COMPARISON RESULTS ON LARGE-SCALE REAL-SCANNED INPUTS

Figure 7 shows more restoration results on large-scale real-scanned inputs (left column) additional to Figure 9 in the main paper, comparing the results of our method (right column) with SampleNet+Dis-PU (middle column). Note that, the input in row (a) is from the outdoor Waymo open dataset [4], while the input in row(b) is from the indoor ScanNet [5] dataset, and row (c) shows the associated reconstructed meshes. Our restored results are significantly much closer to the inputs, *e.g.*, in terms of preserving the original scanlines in (a) and well recovering the details in the inputs in (b), thus promoting an accurate and similar surface reconstruction in (c) as the original.

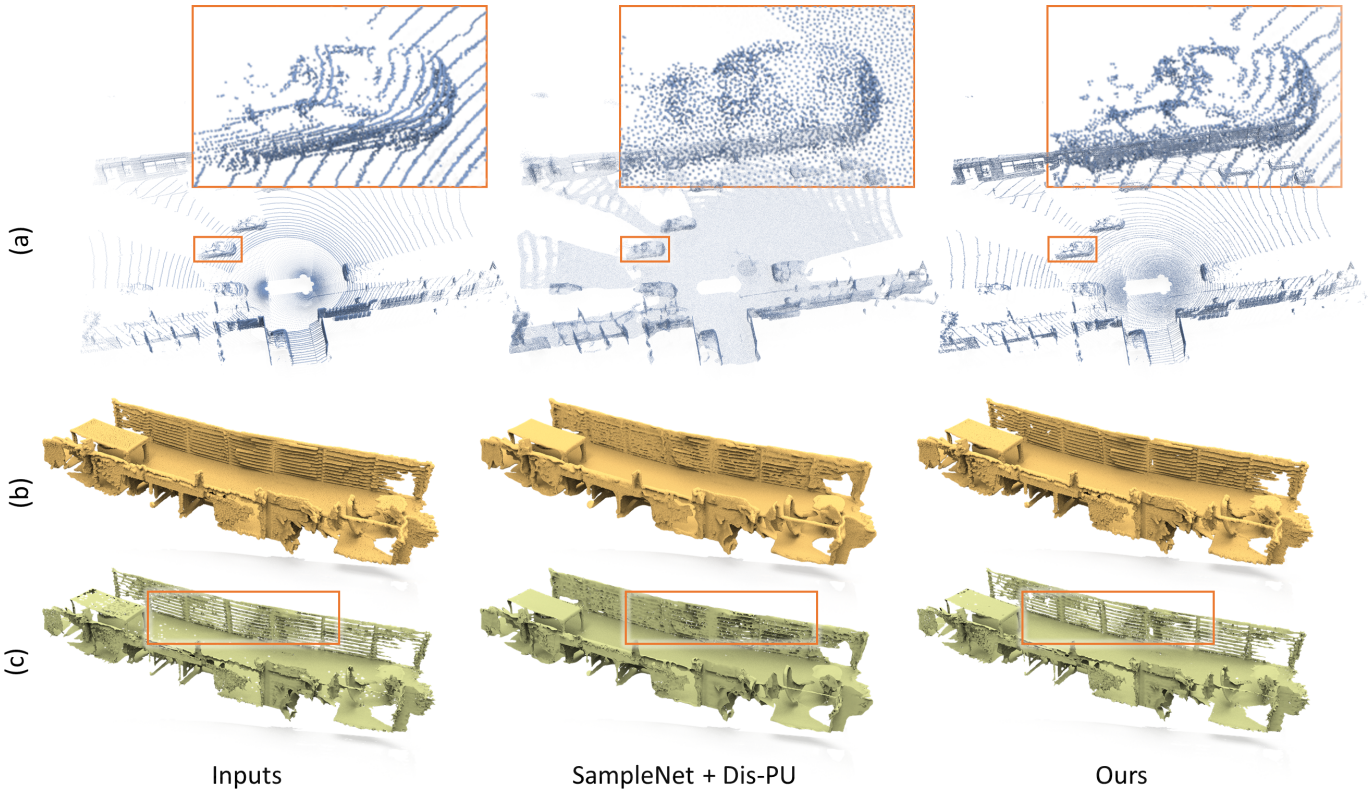


Fig. 7. Restoration results on large-scale real scans. (a) Results on the outdoor Waymo open dataset [4] (b)&(c) Results on the indoor ScanNet [5] and associated 3D reconstructed meshes. Compared with SampleNet+Dis-PU, our results exhibit details that are significantly closer to the inputs.

APPENDIX F
VISUAL COMPARISON WITH POINTLIE

Last, we present a visual comparison between our method and PointLIE [1]. First, note again that for PointLIE, there is no publicly released code so far, so we directly show the visual result from Figure 7 of its original paper [1] on Figure 8(a). Comparing with our result in Figure 8(b), we can see that our result is significantly closer to the inputs, better preserving the original scanlines, whereas PointLIE will smooth out the original details by filling the gaps, similar to the conventional upsampling methods.

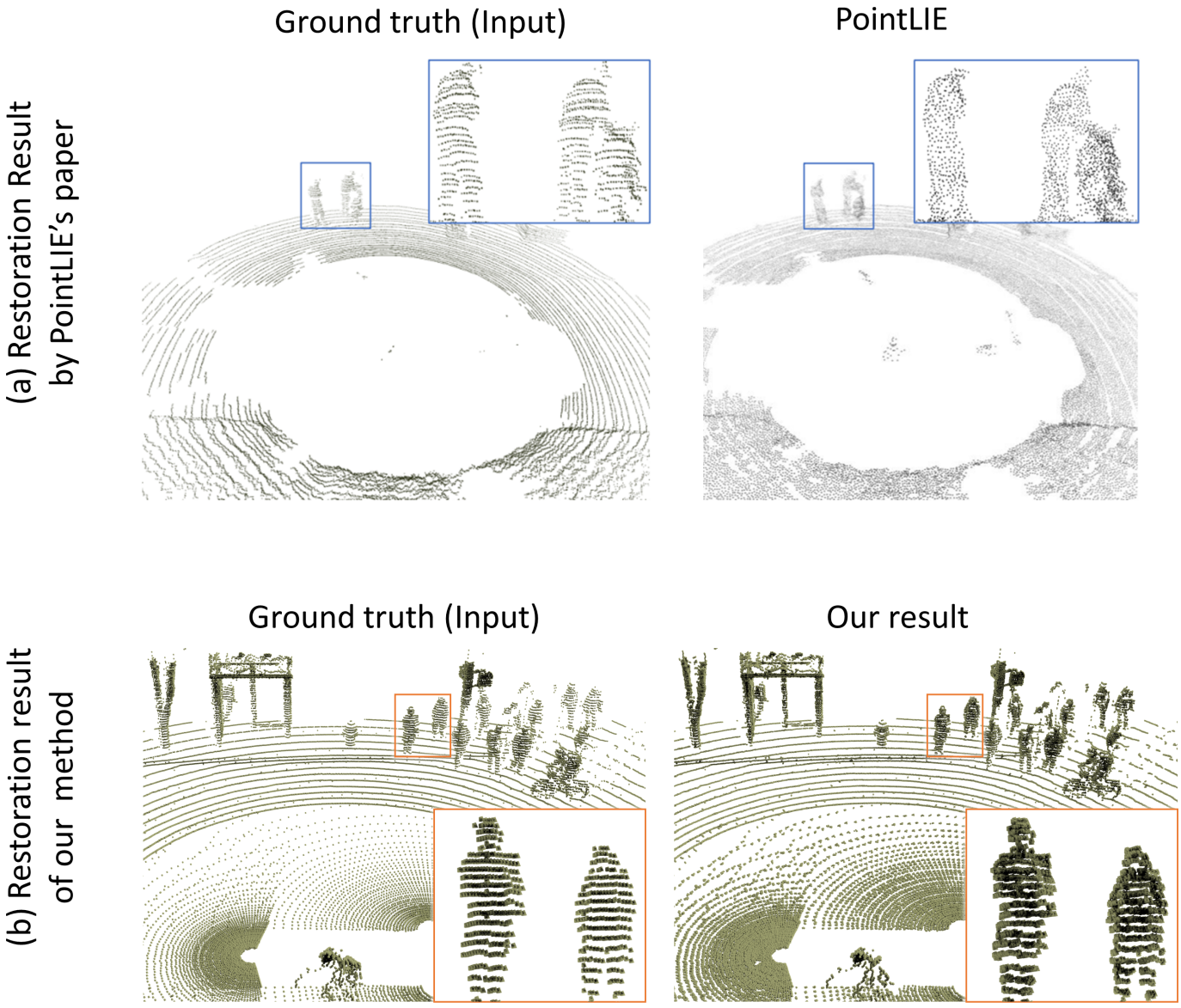


Fig. 8. Restoration on LiDAR inputs. (a): the top row shows a result from PointLIE's paper (the top row is from Figure 7 in PointLIE's appendix); and (b): the bottom row shows a result of our method.

REFERENCES

[1] W. Zhao, X. Yan, J. Gao, R. Zhang, J. Zhang, Z. Li, S. Wu, and S. Cui, "PointLIE: Locally invertible embedding for point cloud sampling and recovery," in *Intl. Joint Conf. on Artificial Intell. (IJCAI)*, 2021, pp. 1345–1351. 1, 9

[2] R. Li, X. Li, P.-A. Heng, and C.-W. Fu, "Point cloud upsampling via disentangled refinement," in *IEEE Conf. on Computer Vision and Pattern Recognition (CVPR)*, 2021, pp. 344–353. 5

[3] I. Lang, A. Manor, and S. Avidan, "SampleNet: Differentiable point cloud sampling," in *IEEE Conf. on Computer Vision and Pattern Recognition (CVPR)*, 2020, pp. 7578–7588. 6

[4] P. Sun, H. Kretzschmar, X. Dotiwalla, A. Chouard, V. Patnaik, P. Tsui, J. Guo, Y. Zhou, Y. Chai, B. Caine *et al.*, "Scalability in perception for autonomous driving: Waymo open dataset," in *IEEE Conf. on Computer Vision and Pattern Recognition (CVPR)*, 2020, pp. 2446–2454. 8

[5] A. Dai, A. X. Chang, M. Savva, M. Halber, T. Funkhouser, and M. Nießner, "ScanNet: Richly-annotated 3D reconstructions of indoor scenes," in *IEEE Conf. on Computer Vision and Pattern Recognition (CVPR)*, 2017, pp. 5828–5839. 8

The End